

LS-DYNA® R7: Conjugate heat transfer problems and coupling between the Incompressible CFD (ICFD) solver and the thermal solver, applications, results and examples.

Iñaki Çaldichoury
Facundo Del Pin

*Livermore Software Technology Corporation
7374 Las Positas Road
Livermore, CA 94551*

Abstract

LS-DYNA version R7 includes CFD solvers for both compressible and incompressible flows. The incompressible CFD solver (ICFD) may run as a stand alone CFD solver for pure thermal fluid problems or it can be strongly coupled using a monolithical approach with the LS-DYNA solid thermal solver in order to solve the complete conjugate heat transfer problem.

This paper will focus on the thermal part of the ICFD solver and its associated features. Several results of thermal and conjugate heat transfer problems will be presented as well as some industrial applications for illustration and discussion purposes.

1- Introduction

LS-DYNA version R7 double precision aims to solve complex multi-physics problems involving fluids, electromagnetism or chemistry interacting with the solid mechanics and thermal solvers of LS-DYNA. This paper will focus on the incompressible flow solver (ICFD) and more specifically on its thermal and conjugate heat transfer capabilities.

Heat transfer is a discipline of thermal engineering that concerns the generation, use, conversion, and exchange of thermal energy and heat between physical systems. The ICFD solver offers the possibility to solve and study the behavior of temperature flow in fluids. Potential applications are numerous and include refrigeration, air conditioning, building heating, motor coolants, defrost or even heat transfer in the human body. Furthermore, the ICFD thermal solver is fully coupled with the thermal solver using a monolithic approach which allows the solving of complex problems where both heated structures and flows are present and interact together.

2- Heat Equation and coupling with the thermal solver for solids

The distribution of heat in a given region of fluid over time is described by a convection-diffusion equation also called heat equation:

$$\frac{\partial T}{\partial t} + u_j \frac{\partial T}{\partial x_j} - \alpha \frac{\partial^2 T}{\partial x_j \partial x_j} = f \text{ in } \Omega$$

where α is the called thermal diffusivity and f is a potential source of heat.

This formulation is incomplete if the appropriate set of boundary conditions and initial conditions is not specified. The user can specify the temperature or the heat flux on the boundaries resulting in Dirichlet or Neumann boundary conditions respectively:

$$T(\vec{x}, t) = T(\vec{x}) \text{ or } \vec{n}(\vec{x}) \cdot \vec{\nabla} T(x, t) = q(\vec{x}) \text{ on } \Gamma$$

Furthermore, if no boundary condition is specified, the solver will automatically apply a Neumann condition:

$$\vec{n}(\vec{x}) \cdot \vec{\nabla} T(x, t) = 0 \text{ on } \Gamma$$

Let us note that, as in accordance with the incompressibility hypothesis, the temperature does not influence the flow's velocity. For specific applications involving free convection, the classic Boussinesq model has been introduced and is available to users.

For the thermal coupling between the heat equation solved by the thermal solver in the structure and the heat equation solved in the fluid by the ICFD solver, a monolithic approach has been adopted. The coupling between the structure and the fluid is therefore very tight and strong at the fluid-structure interface. The resulting full system includes both the structural and the fluid temperature unknowns (See Figure 1) and is solved using a direct solver which may in some cases be computer-time consuming.

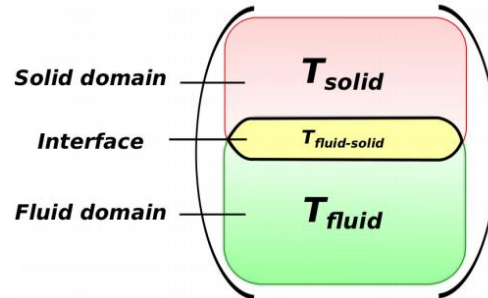


Figure 1 Vector of temperature unknowns when the fluid thermal solver and structure thermal solvers are coupled using a monolithically approach.

3- Validation of the conjugate heat transfer solver

3-1 The analytical solutions

As the development of the different R7 solvers progresses, several verification, validation and benchmarking tests have been conducted both internally at LSTC and externally by beta testing users in order to track bugs and improve numerical accuracy. This section will present some of the results obtained on a conjugate heat transfer problem involving the flow in a parallel plane channel (2D problem) or a cylindrical channel (3D problem).

In [1], the analytical solution of the conjugate heat transfer problem in a parallel plane channel has been studied by applying a periodic temperature boundary condition prescribed on the exterior face of the solid channel ($T = T_0 + \Delta T \sin(\beta z)$). In [2], the problem has been extended to the axi-symmetric cylindrical channel case with a periodic prescribed temperature boundary condition. In all cases, the flow is considered laminar and fully hydrodynamically and thermally developed. Numerous industrial applications meet such conditions and are often encountered in nuclear reactor cooling designs, heat exchangers for Stirling-cycle machines or internally finned ducts. Figure 2 offers a sketch of the complete fluid-solid conjugate heat transfer problem.

As in most fluid mechanics problems, it is often more convenient to work in dimensionless quantities:

$$\eta = y/y_0, \varepsilon = z/z_0, \sigma = y_1/y_0, \theta = \frac{T - T_0}{\Delta T}, \gamma = k_s/k_f, B = Pe\beta y_0, u = U/U_0$$

with y_0 the half height of the internal channel wall, y_1 the half height of the exterior channel wall, z the axial coordinate of the channel, θ the adimensional temperature, k_s and k_f the solid and fluid thermal conductivities respectively, β the angular frequency, U and U_0 the longitudinal component of the fluid velocity and its mean value and finally Pe the Peclet number.

The temperature distribution has been obtained analytically in [1] and in [2] for the 2D and 3D cases respectively by expressing the energy balance equation as a complex-valued hypergeometric confluent equation. The temperature profile can be written as:

$$\theta(\eta, \varepsilon) = \theta_1(\eta) \sin\left(\frac{B\varepsilon}{Pe}\right) + \theta_2(\eta) \cos\left(\frac{B\varepsilon}{Pe}\right)$$

Where it has been shown in [1] that for the 2D case, θ_1 and θ_2 can be expressed as the real and complex parts of the complex valued function:

$$\psi(\eta) = \begin{cases} -C_1 e^{H\eta^2/4} {}_1F_1\left(\frac{2+H}{8}; \frac{1}{2}; -\frac{H}{2}\eta^2\right), & 0 < \eta < 1 \\ C_2 e^{B\eta/Pe} + C_3 e^{-B\eta/Pe}, & 1 < \eta < \sigma \end{cases}$$

where $H = (i - 1)\sqrt{3B}$, ${}_1F_1$ is the confluent hypergeometric function and C_1, C_2, C_3 are complex constants that be calculated using the boundary conditions.

For the 3D case, it has been shown in [2] that the solution can be written as :

$$\psi(\eta) = \begin{cases} C_5 (\Gamma((1-\omega)/2))^{-1} \sqrt{2\omega} \times e^{-\omega\eta^2} \times \sum_{n=0}^{\infty} \frac{\Gamma(n+(1-\omega)/2)}{n! n!} (2\omega\eta^2)^n, & 0 < \eta < 1 \\ C_6 I\left(0, \frac{B\eta}{Pe}\right) + C_7 K\left(0, \frac{B\eta}{Pe}\right), & 1 < \eta < \sigma \end{cases}$$

where Γ is the Gamma function, I and K are the first and second type Bessel functions and $C_5, C_6,$ and C_7 are complex constants that be calculated using the boundary conditions.

Figure 3 offers some examples of temperature distributions for different set of parameters for the 2D case.

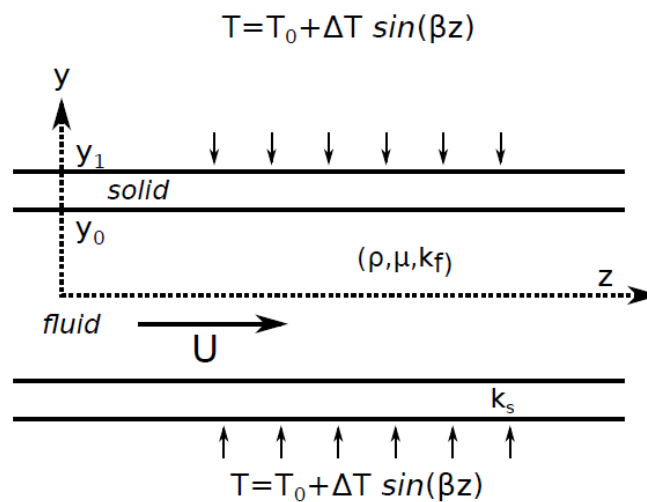


Figure 2 Sketch of the longitudinal section of the channel

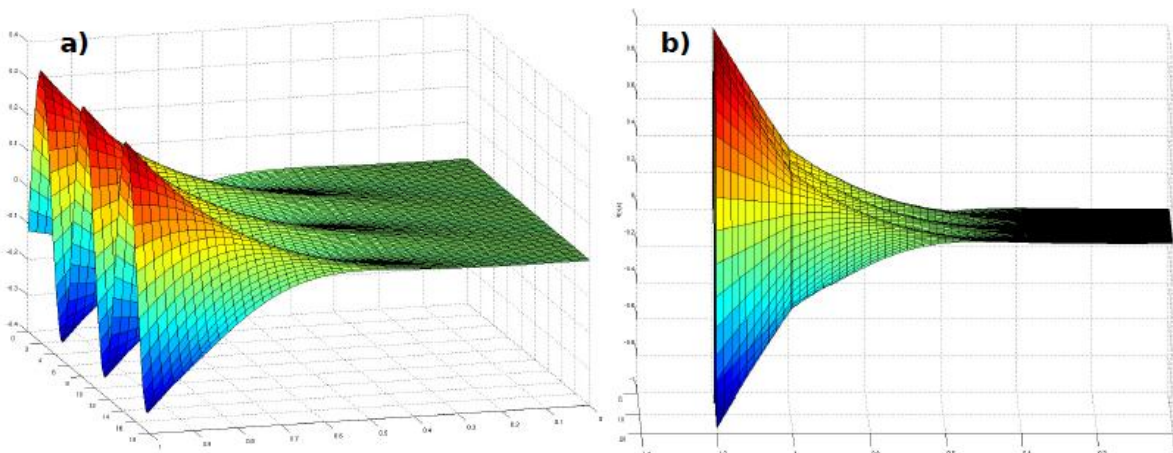


Figure 3 Analytical solution: dimensionless temperature distribution versus η and ϵ for $\sigma = 1.2, B = 100, Pe = 100, \gamma = 0.5$, a) Fluid domain only b) Fluid and Solid coupled domains.

3-1 The numerical solutions

Figure 4 offers a view of the mesh used for both the 2D and 3D cases. For this analysis, several parameters will be varied such as the Peclet number, the angular frequency, thermal conductivities and so forth.

For the 2D case, the continuity of temperature at the interface is well insured by the numerical simulation as can be observed on Figure 5. Figure 6 offers a qualitative comparison between the analytical and the numerical temperature profiles at the solid-fluid interface. In Figure 7a), the dimensionless temperature distribution at the solid-fluid interface is reported and a comparison is made with the analytical solution for different Peclet numbers. A higher Peclet number yields smaller amplitude at the interface. This is consistent as a higher Peclet number value implies more temperature and advection and on the other hand, an infinitely small Peclet number would mean that the fluid has no influence on the solid temperature distribution. Figure 7b), shows that while the period of the axial temperature distribution strongly differs in the three considered cases the oscillation amplitude does not display strong differences. Figure 7c) shows again the dimensionless temperature distribution at the interface for three different values of γ . As expected, a higher γ value yields a temperature distribution closer to the boundary condition profile imposed at $\eta = \sigma$. Finally Figure 7d) shows the temperature profiles at different η along the channel. For all η values, the progressive alignment of the numerical solution with the analytical solution can be observed i.e the progressive establishment of the developed thermal profile. As a conclusion, all figures show an excellent agreement with the analytical solutions.

As for the 2D case, the continuity of temperature between the solid and the fluid can be distinctly observed on Figure 8 for the 3D problem. Figure 9 further confirms the consistent behavior of the numerical solution. As expected, a higher Pe yields a higher temperature amplitude at the interface, a higher periodicity at the boundary impacts the frequency at the interface without impacting the amplitude, a lower thermal conductivity ratio gives a lower temperature at the interface as well as a bigger solid thickness which allows more temperature diffusion through the solid. The numerical solutions are in excellent agreement with the analytical solutions.

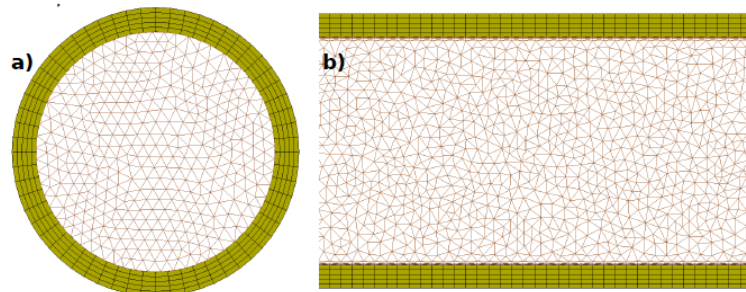


Figure 4 a) 3D surface mesh view, b) 2D mesh view

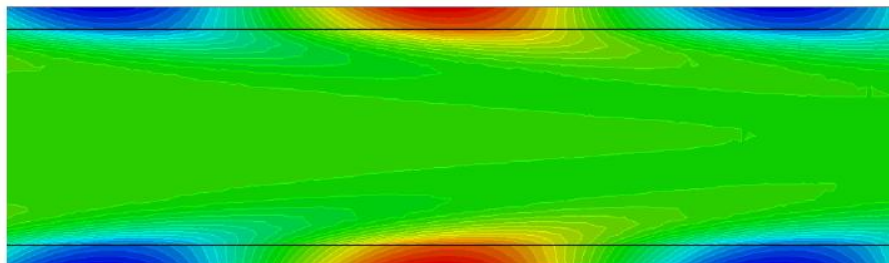


Figure 5 Numerical solution: temperature distribution in the fluid solid domain for $\sigma = 1.2, B = 100, Pe = 100, \gamma = 3$.

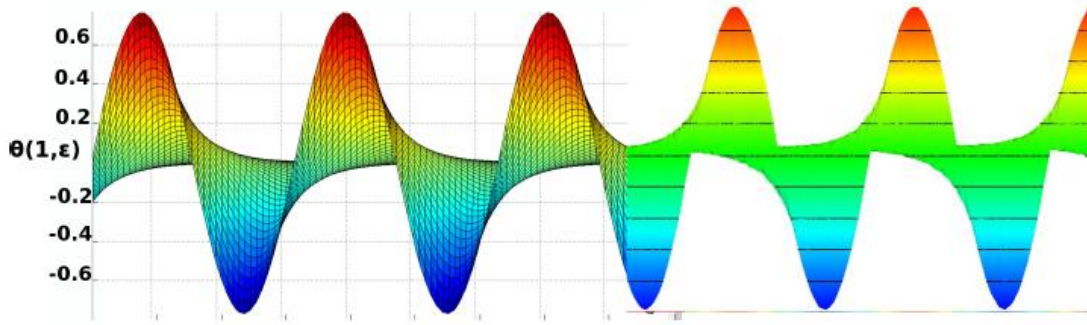


Figure 6 Dimensionless temperature: Qualitative comparison between the numerical and analytical results for the dimensionless temperature at the fluid-solid interface for $\sigma = 1.2, B = 100, Pe = 100, \gamma = 3$.

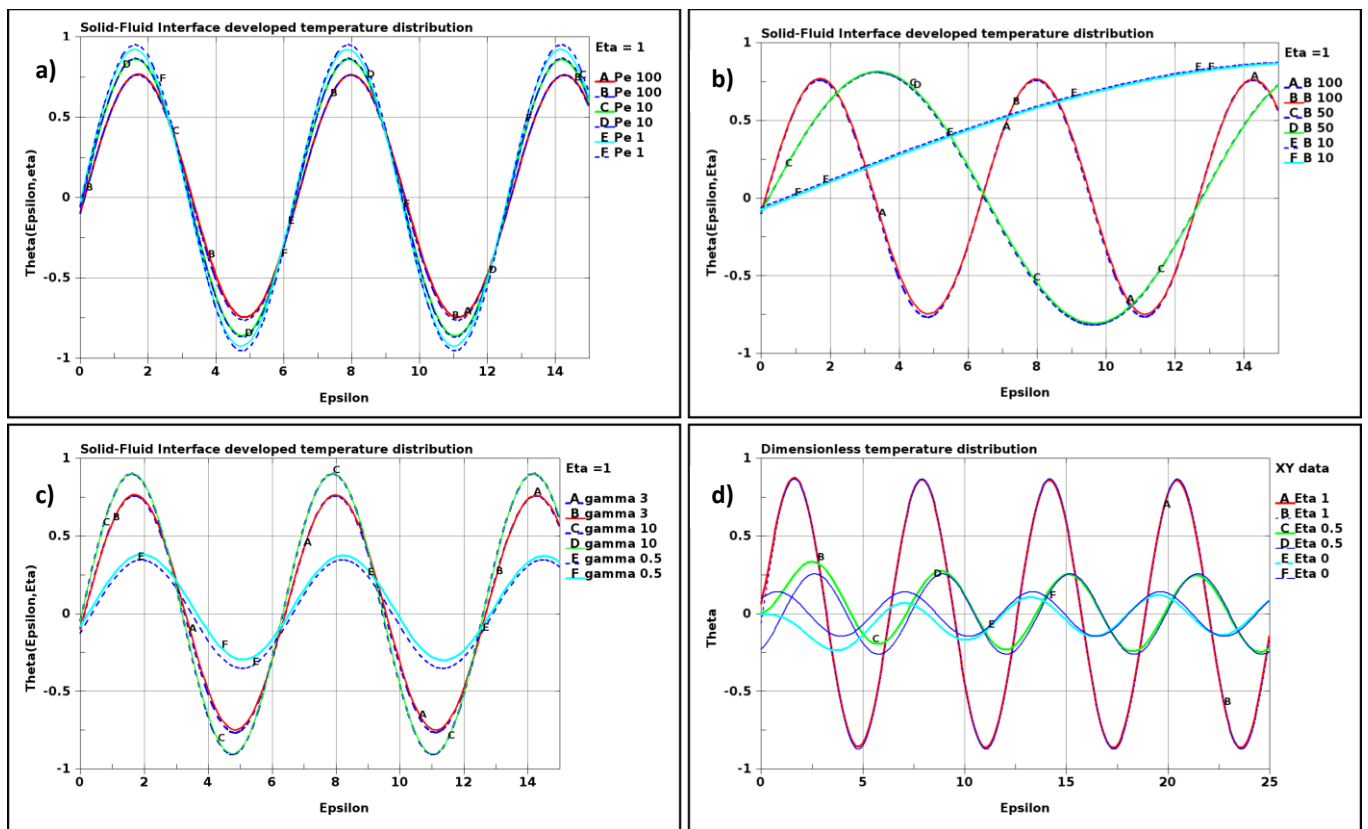


Figure 7 2D case : dimensionless temperature distribution between the analytical solution (in Blue) and the numerical solution: a), b) c) in the hydrodynamically and thermally developed region at the fluid solid interface for a) $\sigma = 1.2, B = 100, \gamma = 3$ and $Pe = 1, 10, 100$, b) $\sigma = 1.2, Pe = 100, \gamma = 3$ and $B = 1, 10, 100$, c) $\sigma = 1.2, B = 100, Pe = 100$ and $\gamma = 0.5, 3, 10$.
 d) Starting from the inlet with $\sigma = 1.2, B = 100, \gamma = 3, Pe = 100$ and $\eta = 1, 0.5, 0$.

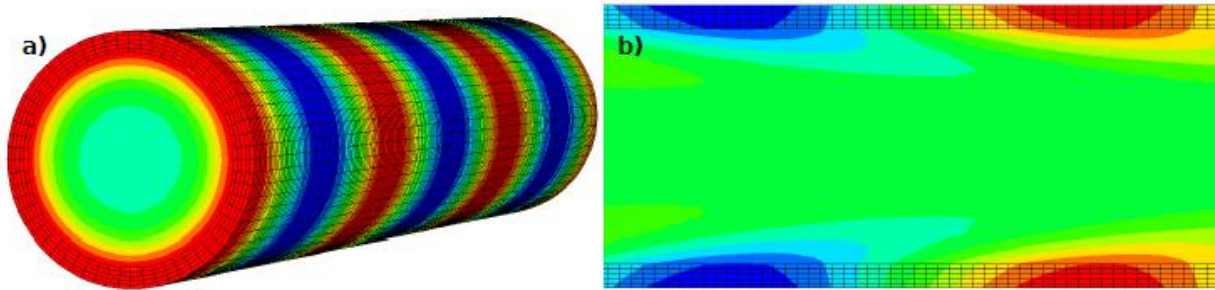


Figure 8 Numerical solution: temperature distribution in the fluid solid domain for $\sigma = 1.2, B = 100, \gamma = 3, Pe = 100$. a) 3D cut view, b) Channel cut view

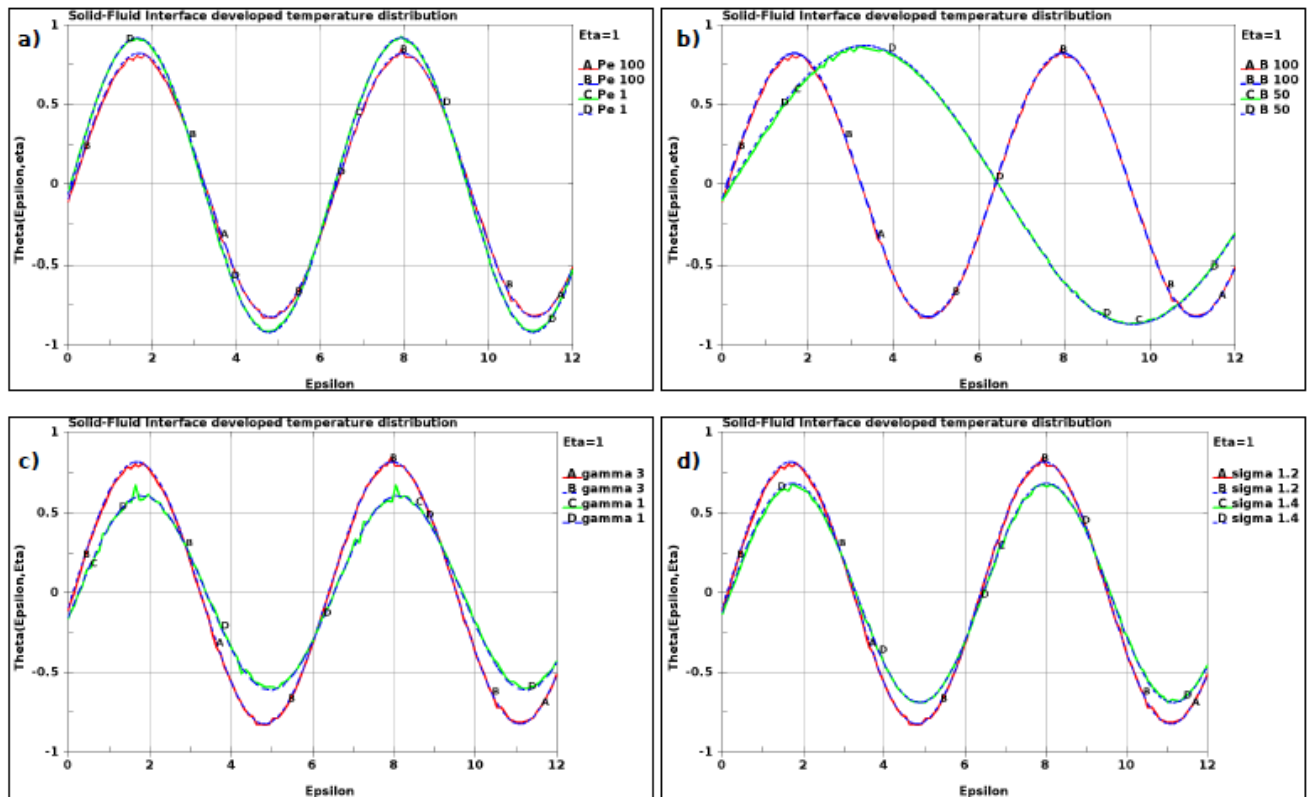


Figure 9 3D case: dimensionless temperature distribution between the analytical solution (in Blue) and the numerical solution: a), b) c) d) in the hydrodynamically and thermally developed region at the fluid solid interface for $\sigma = 1.2, B = 100, \gamma = 3$ and $Pe = 1, 100$, b) $\sigma = 1.2, Pe = 100, \gamma = 3$ and $B = 50, 100$, c) $\sigma = 1.2, B = 100, Pe = 100$ and $\gamma = 1, 3$, d) $\gamma = 3, B = 100, Pe = 100$ and $\sigma = 1.4, 1.2$.

4- Further applications for the conjugate heat transfer solver

As seen previously, the ICFD solver can be used to solve conjugate heat transfer problems involving flow in pipes and cooling of systems and structures. Figure 10 features an example where the solver is being used to solve a stamping application. A workpiece gets stamped against the die, and the fluid flowing through a snake shaped pipe through the die is responsible for the subsequent cooling of both the workpiece and the die. Figure 11 shows another example of a problem currently under investigation where the conjugate heat transfer solver is being used to solve a coupled problem involving the thermal and the

EM solvers. Due to the Electromagnetic Joule heating, a sparse coil gets heated up and the flow running through the center of it is used to cool it down in order to prevent it from melting.

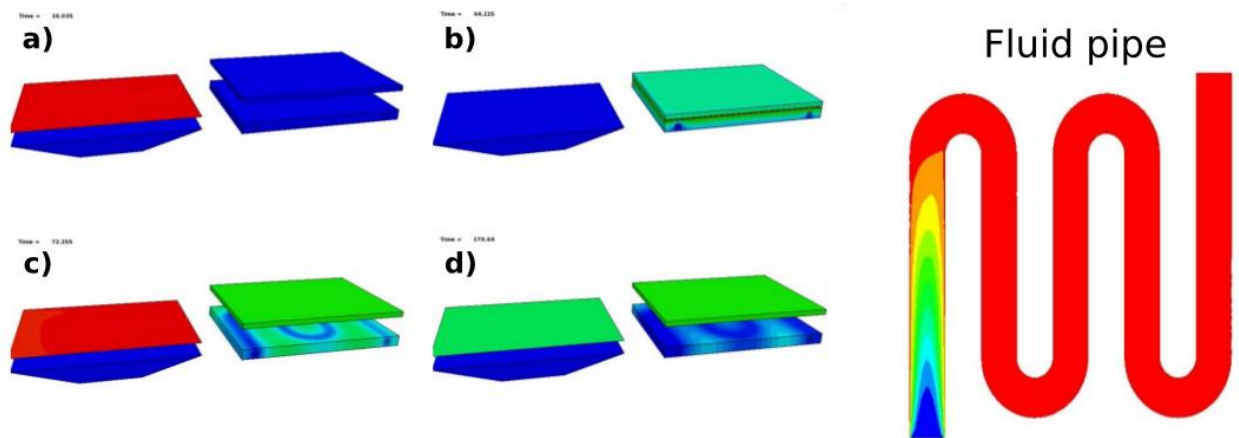


Figure 10 Stamping application, temperature fringes: a) Initial state with hot workpiece b) Workpiece moved to the right and pressed against the die. Coolant liquid flowing through the die active. c) Workpiece moved back to initial position. Cooling of the die and the workpiece. D) Final state, cooled workpiece and die.

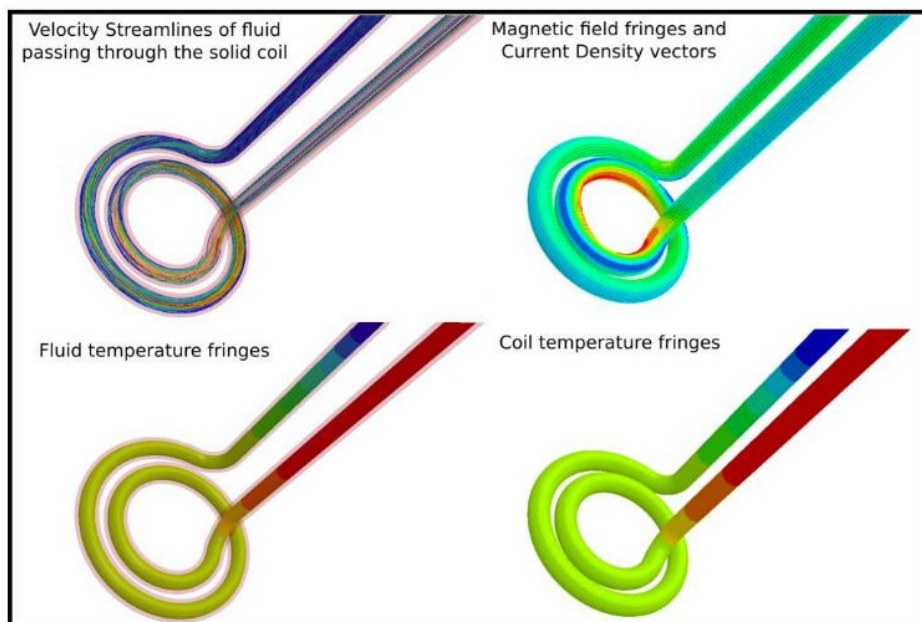


Figure 11 Coupled EM-thermal-ICFD application: Cooling of coils used for induced heating applications

References

- [1] A. B. a. E. D. S. a. G. C. a. P. D'Agaro, «Conjugate forced convection heat transfer in a plane channel : Longitudinally periodic regime,» *International Journal of thermal Sciences*, n° 47, pp. 43-51, 2008.
- [2] M. R. A. a. N. Tabari, «Two dimensional analytical solution of the laminar forced convection in a circular duct with periodic boundary condition,» *Journal of thermodynamics*, 2012.